

NATURAL CONVECTION FROM WALL SECTIONS OF ARBITRARY TEMPERATURE DISTRIBUTION BY AN INTEGRAL METHOD

MAX G. SCHERBERG

Thermo-Mechanics Research Laboratory, Aerospace Research Laboratories, Office of Aerospace Research, United States Air Force, Wright-Patterson Air Force Base, Ohio

(Received 2 January 1963 and in revised form 30 December 1963)

Abstract—Solutions are found for the natural convective flow from sections of vertical plates having suitably restricted arbitrary wall temperatures so that temperature and speed distributions in the flow have similarity forms of the type found in the constant wall temperature case. Several cases are studied in detail in which streamlines, isotherms, and speed distributions are disclosed. Included are cases of increasing-decreasing temperature sections and the converse. Also studied are the heat transfer and other effects of varying the initial or starting conditions on the wall sections.

NOMENCLATURE

ρ_{∞}	ambient gas density [lb/ft ³];
T_{∞}	ambient absolute temperature [°R];
δ_0	boundary layer starting thickness [ft];
u_0	speed function starting value [ft/s];
T	absolute temperature [T_{∞} units];
ν	kinematic viscosity [$(u_0 \cdot \delta_0)$ units];
Pr	Prandtl number;
x, y	vertical and horizontal coordinates respectively [δ_0 units];
δ	boundary-layer thickness [δ_0 units];
η	$1 - y/\delta$;
τ	temperature function [$T = 1 + \tau\eta^2$];
u	speed function [$U = u(\eta^2 - \eta^3)$], [u_0 units];
U	vertical convective speed [u_0 units];
S	relative volume flow rate [$u\delta$];
R_s	standards ratio [$(u/\delta^2)/(u\delta^2)_{st}$];
$(U/\delta^2)_{ST}$	$1.75 g\tau Pr / [\nu(S + 5.25 Pr)]$;
N	Nusselt number;
g	acceleration of gravity [(u_0^2/δ_0) units];
ρ	gas density [ρ_{∞} units];
w	subscript to denote wall conditions.

conventional integral momentum-energy boundary-layer equations for natural convection from a heated vertical plane surface

$$-\int_0^{\delta} (1 - \rho) dy + \frac{d}{g dx} \int_0^{\delta} \rho U^2 dy + \nu \left(\frac{\partial U}{\partial y} \right)_w = 0,$$

$$\frac{d}{dx} \int_0^{\delta} \rho U (T - 1) dy + \frac{\nu}{Pr} \left(\frac{\partial T}{\partial y} \right)_w = 0$$

may be reduced to ordinary differential equations in the independent variable x of the form

$$\tau' u \delta^2 + \tau (u' \delta^2 + u \delta \delta' - c_2) = 0, \quad (1)$$

$$2uu' \delta^2 + u^2 \delta \delta' - c_3 \tau \delta^2 + c_4 u = 0 \quad (2)$$

in which the primes indicate differentiation with respect to x and $c_2 = 60\nu/Pr$; $c_3 = 35g$; $c_4 = 105\nu$ if one seeks solutions of the form

$$U = u(x) (\eta^2 - \eta^3), \quad \eta = 1 - y/\delta. \quad (4)$$

$$T = 1 + \tau(x)\eta^2. \quad (5)$$

It was pointed out that these assumed solution forms first used by Squire [2] for the constant wall temperature case provide the required boundary conditions $U = 0$, $T = 1 + \tau(x)$ at the wall and $U = 0$, $T = 1$ at the edge $y = \delta$ of the boundary layer. It was shown that such

It was shown in reference 1 that the following

INTRODUCTION

solutions for the variable wall temperature distributions defined by $\tau = px^n$, p and n constants and $n > 1$ compare acceptably with results in reference 3 which used the traditional Pohlhausen method. It was further shown that for the constant wall temperature case the equations (1) and (2) may be solved with arbitrary initial conditions u_0 , δ_0 at some starting position on the plate, and that the essential characteristics of the boundary layer at an adequate distance above the starting point are independent of the starting values u_0 , δ_0 . In fact, it was found that variations in u_0 , δ_0 have only the effect of giving the upper boundary-layer variations in vertical position relative to the wall. It was pointed out that if u_0 , δ_0 were selected so that

$$1.75 g\tau Pr/\nu(5 + 5.25 Pr) = 1$$

then the solution of equations (1) and (2) is equivalent to the Pohlhausen solution if we compare it with the latter beginning with a value of $x = x_0$ in the latter at which $u = 1$ and $\delta = 1$. In this paper, the vertical displacement effect of the starting values u_0 , δ_0 are computed as a function of these values.

The solution of equations (1) and (2) with arbitrary starting values u_0 , δ_0 when τ is constant enables one to treat the variable wall temperature case by a partition process. At the moment, it is felt that the cases should be restricted to wall temperatures high enough above ambient so that essentially vertical isotherms may be anticipated in the flow and the wall temperature gradients should be small enough to allow the use of a mean constant local wall temperature in small segments of the wall. The constant wall temperature closed form solution, given in this paper, makes the above application particularly feasible and discloses some parametric forms which should give a better feel for the flow phenomena involved.

Five variable wall temperature cases are studied. Three were taken to match the experimental data of reference 6 and two include the presence of both positive and negative wall temperature gradients.

CLOSED FORM SOLUTION OF CONSTANT TEMPERATURE CASE

The equations (1) and (2) were derived and

solved by asymptotic series expansions for the case $\tau' = 0$ in reference 1. They have since then been solved for that case in the closed form:

$$u = S^{2/3} [1 + E_0 S^{-P}]^{1/3} / R_0^{1/3} \quad (6)$$

$$\delta = S^{1/3} R_0^{1/3} / [1 + E_0 S^{-P}]^{1/3} \quad (7)$$

$x - x_0 =$

$$R_0^{1/3} Pr \left[\int_1^S S^{1/3} dS / (1 + E_0 S^{-P})^{1/3} \right] / 60\nu \quad (8)$$

in which

$$S \equiv u\delta \quad (9)$$

$$R \equiv (u/\delta^2) / (u/\delta^2)_{St} = 1 + S^{-P} E_0$$

$$R_0 \equiv 1 / (u/\delta^2)_{St} = 1 + E_0$$

$$(u/\delta^2)_{St} \equiv (u/\delta^2)_{\text{standard}} \equiv 1.75 g\tau Pr/\nu P$$

$$P \equiv 5 + 5.25 Pr.$$

There are a number of interesting points about this solution. Since the velocity U has the similarity form shown in equation (4), the parameter S represents a volume flow growth factor on the starting volume flow. The ratio factor R_0 represents the excess ratio of the value of u/δ^2 at the starting position over the fixed value $(u/\delta^2)_{St}$ of the Pohlhausen solution. For the latter, $R = R_0 = 1$. It is clear that as the volume flow increases R approaches one and the boundary-layer characteristics approach those of the Pohlhausen solution. If at the starting position, $R_0 = 1$ so that the additive excess $E_0 = 0$, then $R \equiv 1$ and the flow characteristics start and remain those of the Pohlhausen solution.

It has been indicated that the boundary layer ultimately acquires the flow characteristics of the Pohlhausen solution above the starting position, but the vertical position of this flow relative to the wall definitely depends on the starting values u_0 , δ_0 . The vertical position effect may be computed as follows:

When S is sufficiently large, then

$$u = S^{2/3} / R_0^{1/3} \quad (10)$$

$$\delta = S^{1/3} R_0^{1/3}$$

and from the integrated series expansion of the integrand in equation (8):

$$x - x_0 = \{S^{4/3} - 1 + E_0/[3(1 - 3P/4)]\} R_0^{1/3} Pr / 80\nu \quad (11)$$

If we set

$$\bar{x} - x_0 = \{1 - E_0/[3(1 - 3P/4)]\} R_0^{1/3} Pr/80 \nu$$

then equation (11) becomes

$$x + \bar{x} = R_0^{1/3} Pr S^{4/3}/80 \nu \tag{12}$$

and equations (10) and (11) reduce to

$$\left. \begin{aligned} u &= [(x + \bar{x}) 560 \tau g / (20 + 21 Pr)]^{1/2} \\ \delta &= [(x + \bar{x}) 80 \nu (20 + 21 Pr) / 7 Pr g \tau]^{1/4} \\ x_0 + \bar{x} &= \frac{1}{80} \left[\frac{(20 + 21 Pr) Pr^2}{7g \tau \nu^2} \right]^{1/3} \\ &\quad \times \left[1 + \frac{E_0}{8.25 + 11.8125 Pr} \right] \\ &= \frac{1}{140} [P/R_0^{2/3} g \tau] \\ &\quad \times \left[1 + \frac{E_0}{8.25 + 11.8125 Pr} \right] \end{aligned} \right\} \tag{13}$$

in which \bar{x} is the effective vertical displacement position above the normal position of the Pohlhausen solution. It is interesting to note that if one selects the arbitrary position x_0 as zero, and, if further, u_0, δ_0 are such that $R_0 = 1$, then the displacement increment \bar{x} corresponds to the x value in the Pohlhausen solution where $u = 1, \delta = 1$. Of course, if $R_0 \neq 1$, then the \bar{x} cannot be so related. On the other hand, it is clear from equation (13) that \bar{x}, τ and Pr may be fixed and u_0 determined as a function of R_0 for the fixed set. Thus, there are many initial values or starting conditions leading to the same boundary layer at a sufficient distance from the initial point, and it is clear that the upper boundary layer is not uniquely related to a specific set of initial conditions. It is also clear on the other hand that the vertical position of the upper boundary layer does, in general, depend on the starting conditions.

It should be remembered that even though the presence of non-standard initial values $u_0 \delta_0$ do not affect the ultimate u, δ forms of the boundary layer that this is not the case for values of x near x_0 .

VARIABLE WALL TEMPERATURE CASES STUDIED

As has been indicated above, the constant wall temperature results with arbitrary initial conditions may be used in a piece-wise manner to study some variable wall temperature case for which the similarity forms, (4) and (5), are admissible and the isotherms remain essentially vertical. The following wall temperature distributions have been studied in some detail.

Case	Wall temperature distribution
I	$T_w = 1.03056 + 0.137678 (x/100)$
II	$T_w = 1.118182 - 0.413091 (x/100)^2$
III	$T_w = 1.183251 - 0.183251 (x/100)^{1/2}$
IV	$T_w = 1.118182 + 6.28264 (x/100)^2$ $+ 29.32364 (x/100)^3$ $+ 33.97818 (x/100)^4$
V	$T_w = 1.118182 - 6.28364 (x/100)^2$ $- 29.32364 (x/100)^3$ $+ 33.97818 (x/100)^4$

The first three cases were taken because they represented experimental temperature distributions reported in reference 6.

Cases IV and V, on the other hand, are exploratory cases in which respectively the wall temperature decreases about 40° and then increases back to the starting temperature, and where contrariwise, there is first an increase of 40° and a decrease back to the starting temperature.

NUMERICAL PROCEDURES

Although the solutions (6), (7) and (8) are in closed form, the values of u and δ are not available explicitly as functions of x and use of the parameter S must enter the calculations. The procedure was as follows: A starting position somewhere on the wall must be selected and starting values of u_0 and δ_0 estimated in some manner, from say some measured data, or for the purpose of exploratory determinations. The equations (6) and (7) then determine u and δ in a constant temperature step above and/or below the starting position. Equation (8) determines a length or distance from the starting position on the wall for the temperature step. The parameter S is restricted so as to make the constant temperature assumption plausible and so that

further decreases in the size of the step do not yield significant increases in accuracy of the step routine. At the terminal position for the step, we will have values for u , δ and T_w which are used as starting values for the next step and so the calculations progress from the original starting position. They may be continued so long as the equation forms (4) and (5) remain admissible and the simplifying assumption leading to the applied boundary-layer equations remain valid.

CORRECT FOR THE ASSUMPTION OF CONSTANT PROPERTIES

In order to compensate in part for having assumed constant kinematic viscosity in the boundary-layer equations, a mean constant value $\bar{\nu}$ for each temperature step was determined from the equation

$$\int_1^3 \nu (\partial^2 U / \partial y^2) dy = \bar{\nu} \int_0^3 (\partial^2 U / \partial y^2) dy \\ = - \bar{\nu} (\partial U / \partial y)_y = 0 \quad (15)$$

It turns out the mean value $\bar{\nu}$ so determined is that value of ν corresponding to the temperature T at $y = \delta/6$. A better estimate for the viscosity factor $\bar{\nu}$ would have been obtained if a mean value of μ had been determined by equation (15) in place of ν since the ν of the coefficient c_4 in equation (2) should be $\bar{\mu}/\rho_\infty$. It may be shown that a mean $\bar{\mu}$ also occurs at $y = \delta/6$. It is not expected that improved estimates of these constants if one also includes Pr would influence the general information found for the cases studied and so a study of such corrective effects was not undertaken at this time.

DISCUSSION OF RESULTS

As has been indicated, the first three temperature distribution cases were taken to match those in reference 6 in the hopes of having an experimental check on the analytical method developed by this paper. It was hoped that although check u values were not available, some exploratory determinations would lead to appropriate necessary starting values so that comparisons would be available on other values involved. Efforts to obtain values of the variation of δ from the optical data of the reference with an adequate degree of accuracy turned out to be

rather hopeless so that all the retained was a comparison with the experimentally determined heat-transfer coefficient N .

When it became clear that starting δ 's could not be accurately estimated from the photographed optical data of reference [6], it was decided that what appeared to be a good mean starting value of $\delta_0 = 0.04$ ft would be used for most of the calculations. Again, since no values of u were available, it was decided to run exploratory calculations with variation on the parameter R , since $R = 1$ defines the classical Pohlhausen solution for the constant temperature case.

Case I

Figure 1 shows the computed data for Case I in which the temperature varied linearly from $T_w = 1.03056$ at the bottom starting point to $T_w = 1.08490$ at $x = 39.5$ ft an upper point. Two upper curves show variations in R from respective starting values of $R_0 = 0.406$ and $R_0 = 1$. The values soon become almost equal and remain less than 1, but not markedly so. This indicates that always either δ is slightly greater and/or u is slightly smaller than the corresponding values ($R = 1$) for a constant temperature plate at the temperature corresponding local temperature on the plate studied. The N curve shows the variation in heat-transfer coefficient computed with starting values of $\delta_0 = 0.04$ ft and $R_0 = 1$. The lower δ curves show the effect of variations in the starting R values. It appears, as far as δ is concerned, that at a suitable distance from the starting point the effect becomes, as in the case of the constant temperature plate, just a vertical displacement.

The experimental N values of reference 6 were markedly higher than the computed values as shown in Fig. 1. These data were also compared with computed N values for constant temperature plates corresponding to the highest and lowest temperatures of Case I. Since such computations for constant temperature plates (only values at $x = 20$ shown in Fig. 1) have well established accuracy and since these results also showed the experimental data to be too high, it was felt that comparisons of the current calculations with these experimental data were not suitable.

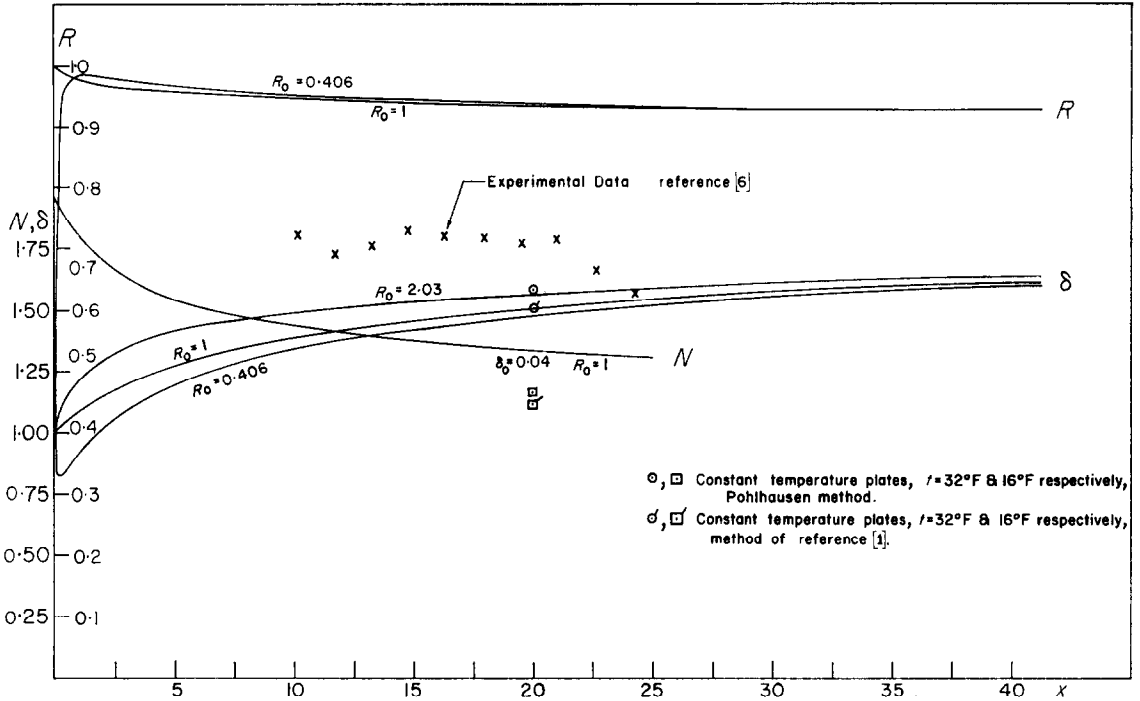


FIG. 1. Case I. Uniformly increasing wall temperature δ , R and N functions.

Case II

Figure 2(a) shows the assumed temperature distribution for that case and the variations in u for starting R values of 2.5 and 0.75 when the δ_0 starting value is 0.04. For $R_0 = 2.5$, it is seen that the u decreases from 1 for a short distance and then goes into an increasing range. The starting fluid is moving too fast for the upper fluid and is decelerated because of restricted access space. Figure 2(c) shows correspondingly a rapid thickening of the boundary layer in the starting region. Again, in Fig. 2(a), it is interesting to note relatively small variations in u , and an approximately uniform speed corresponding to about $u = 1$ when $R_0 = 2.5$. In Fig. 2(b), we note that the R values rapidly approach the standard value 1 and then gradually increase on the upper part of the plate to about 1.4. The computed heat-transfer coefficients differ markedly from those reported [6] in the starting region. Based on the experience with these calculations, it is almost certain that the agreement would have been much better

if a starting $\delta_0 = 0.02$ had been used in place of $\delta_0 = 0.04$. Since the reported heat-transfer coefficients [6] did not come from direct heat-transfer measurement but were computed from readings from photographed interferograms (which apparently the present writer did not read the same way), it was considered questionable of value at this time to attempt to fit this data more closely with the present calculations. Figures 2(c) and 2(d) show the streamline structures corresponding to the starting values $R_0 = 2.5$ and $R_0 = 0.75$, respectively. It has already been observed that the higher starting speed corresponding to $R_0 = 2.5$ results in a sudden thickening of the boundary layer in the starting region. We may also note a slight wave form in the streamlines and that they are concave to the wall in the starting region. For $R_0 = 0.75$, the boundary layer shows a starting contraction indicating that the starting speed value u_0 is too low for the speeds above so that the starting flow is sucked up, so to speak, by the faster motion above. It is also noted that

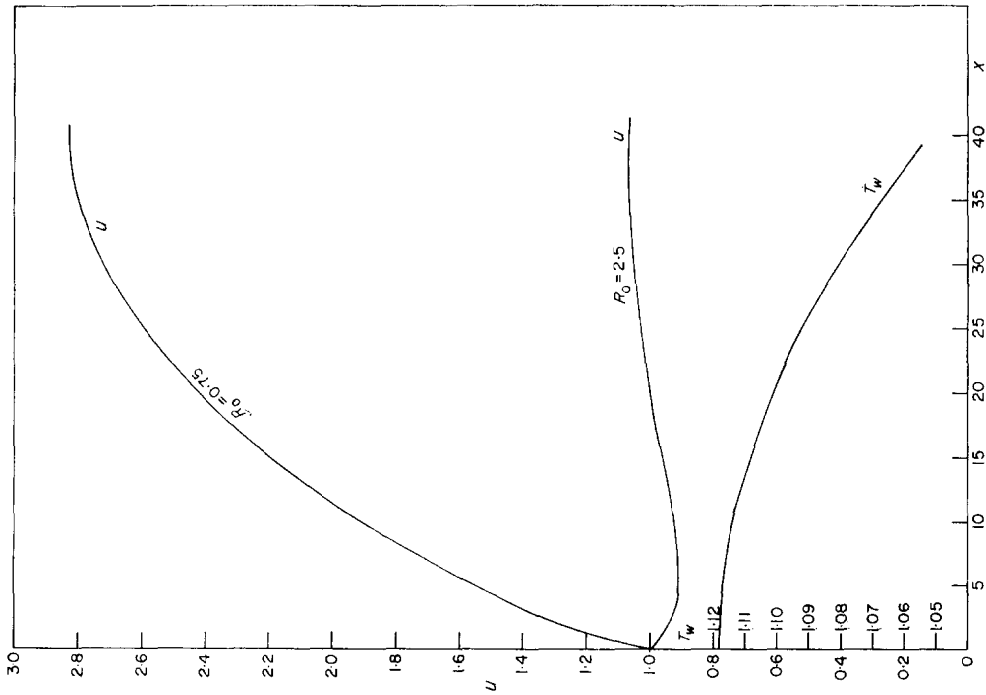


FIG. 2(a). Case II. Decreasing wall temperature, speed functions.

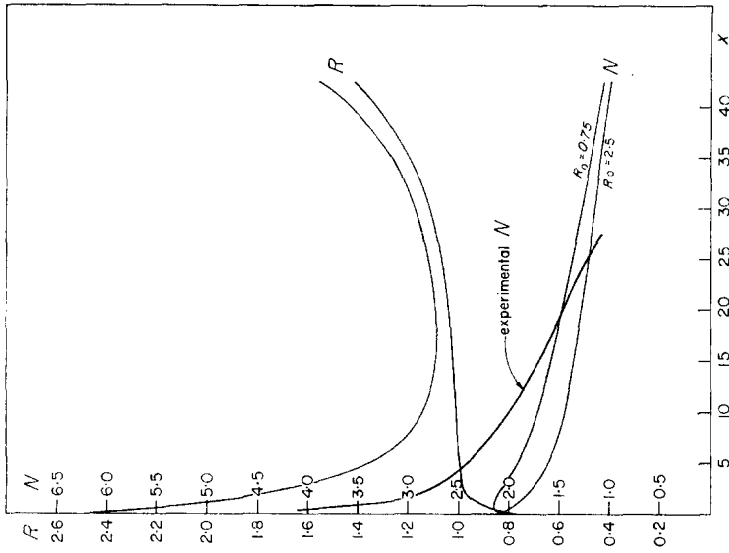


FIG. 2(b). Case II. Heat transfer and R functions.

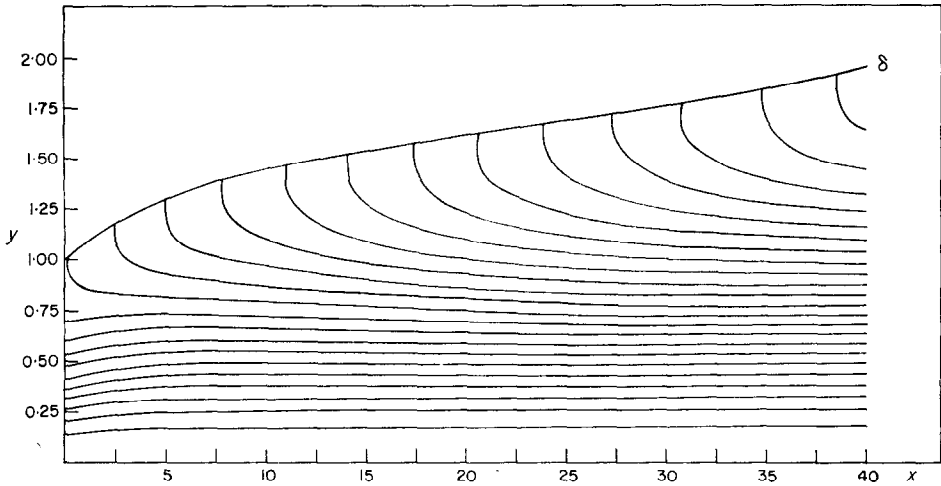


FIG. 2(c). Case II. Streamlines ($R_0 = 2.5; \delta_0 = 0.04$).

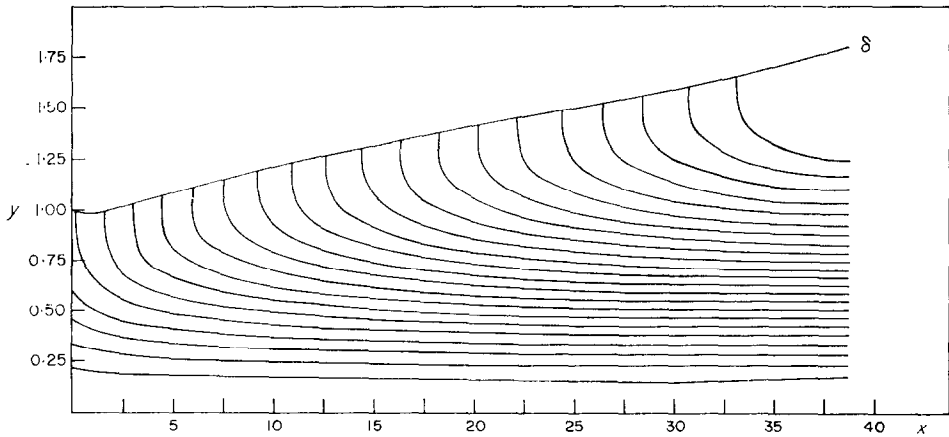


FIG. 2(d). Case II. Streamlines ($R_0 = 0.75; \delta_0 = 0.04$).

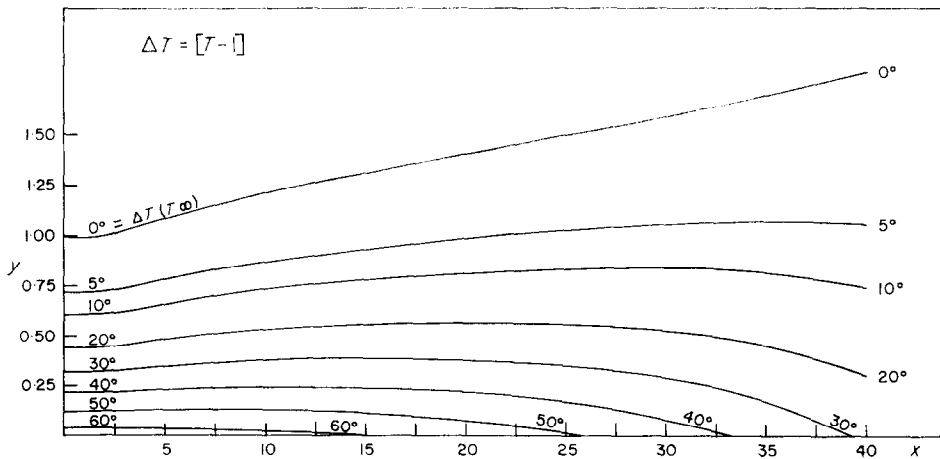


FIG. 2(e). Case II. Isotherms ($R_0 = 0.75; \delta_0 = 0.04$).

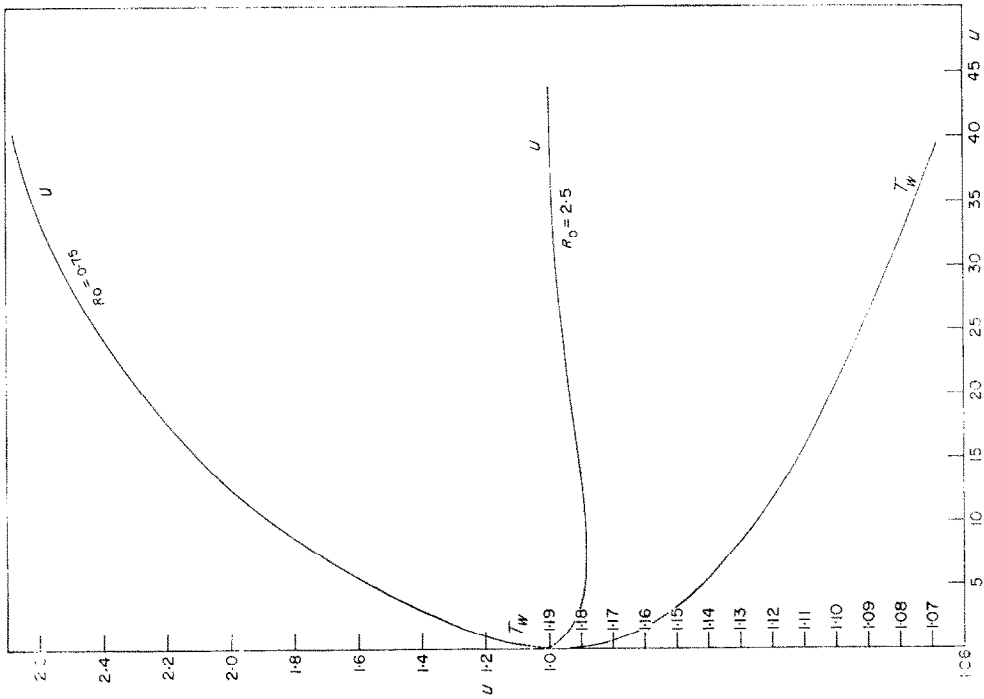


Fig. 3(a). Case III. Temperature and speed functions.

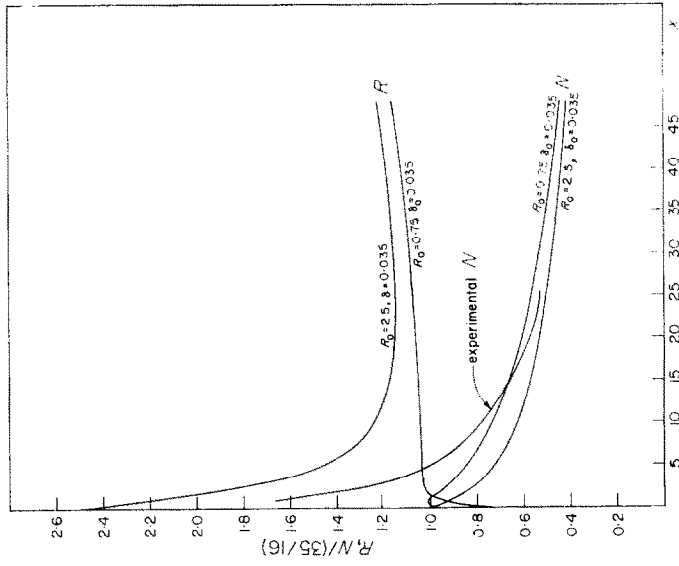


Fig. 3(b). Case III. Heat transfer and R functions.

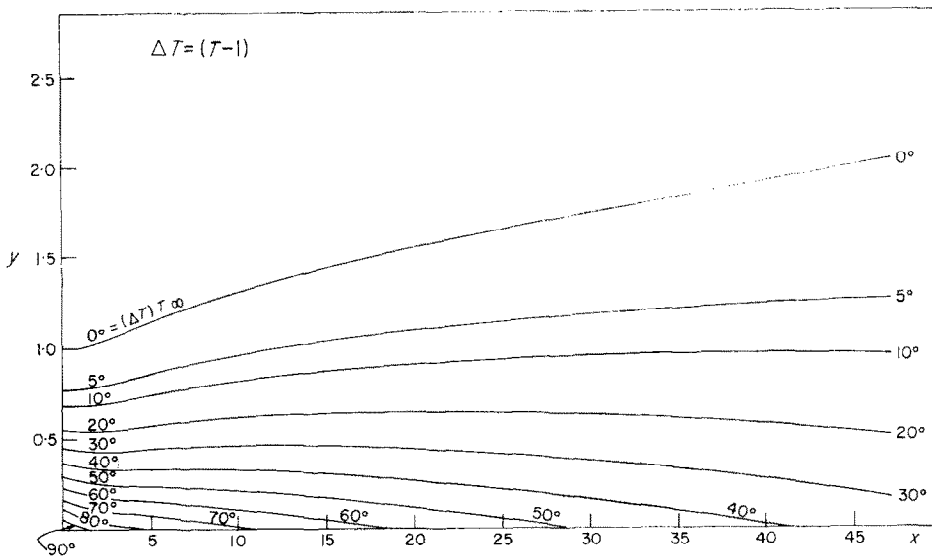


FIG. 3(c). Case III. Isotherms ($R_0 = 0.75$; $\delta_0 = 0.35$).

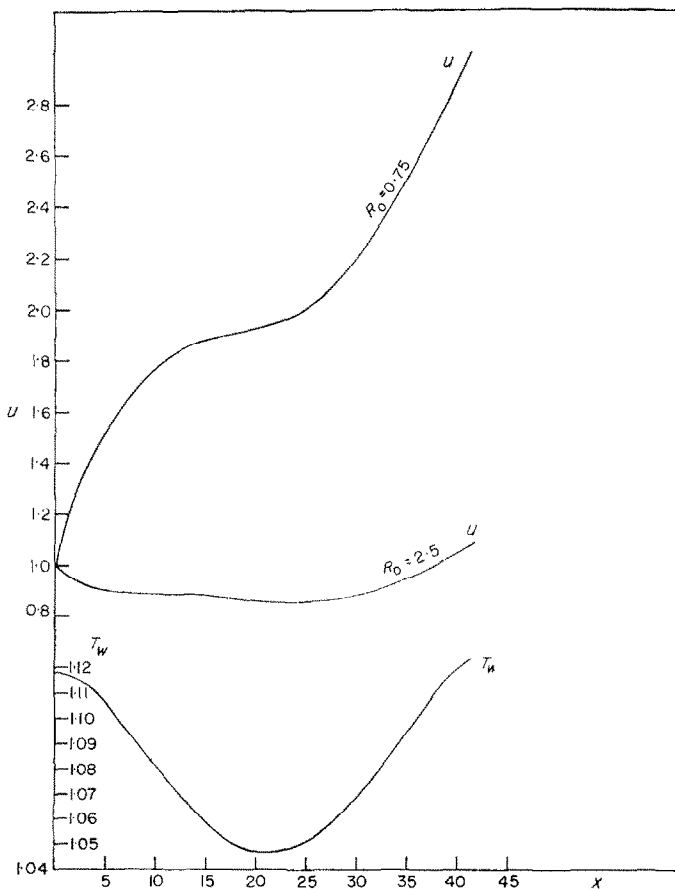


FIG. 4(a). Case IV. Temperature and speed functions.

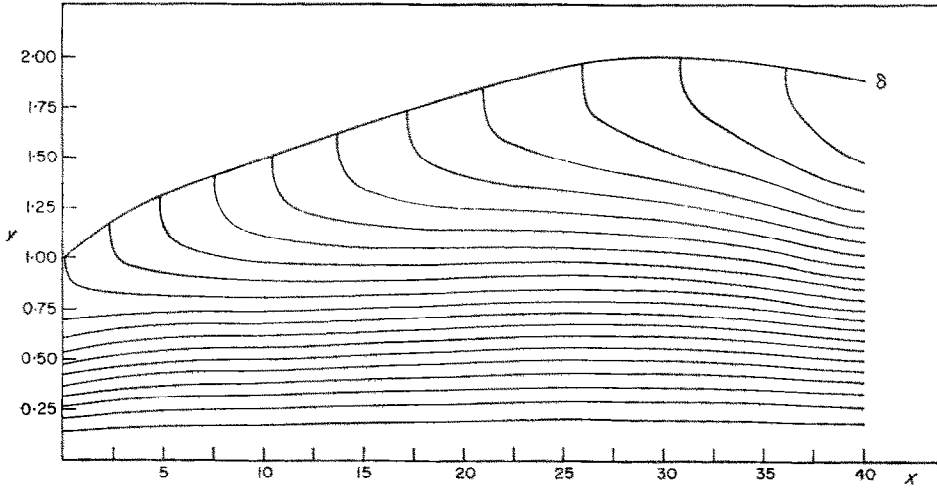


FIG. 4(b). Case IV. Streamlines ($R_0 = 2.5$).

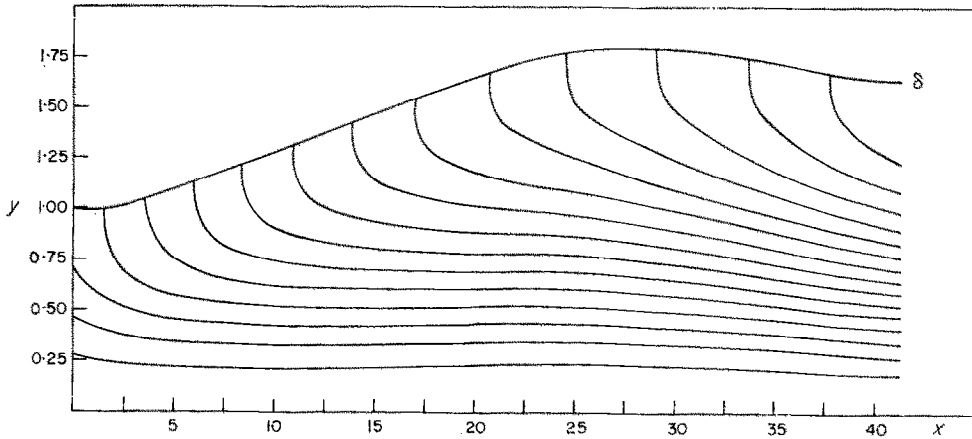


FIG. 4(c). Case IV. Streamlines ($R_0 = 0.75$).

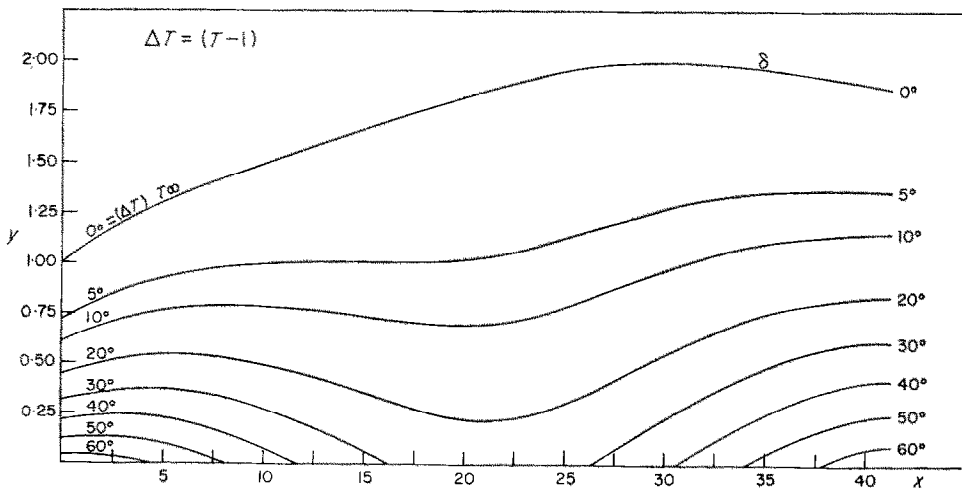


FIG. 4(d). Case IV. Isotherms ($R_0 = 2.5$).

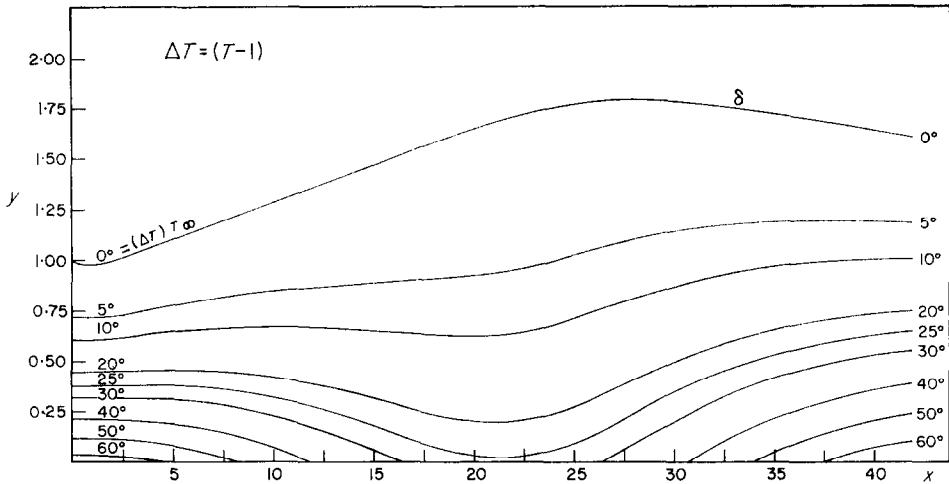


FIG. 4(e). Case IV. Isotherms ($R_0 = 0.75$).

streamlines are convex to the wall which would be conducive to the formation of Gortler vortices and possible early flow instability. Figure 2(e) shows the isotherm structure for the value $R_0 = 0.75$. The relatively rapid thickening of the lower temperature outer layer of the boundary layer, probably resulting from the decreasing temperature on the wall, is of interest.

Case III

Some of the flow characteristics for this case are shown in Figs. 3(a), (b) and (c). The starting values were $\delta_0 = 0.035$, $R_0 = 2.5$ and $R_0 = 0.75$. The results are not significantly different in form from those of Case II and do not need general discussion. It may be noted that in this case the R values are closer to 1 on the upper plate region.

Case IV

In Fig. 4(a), we note that the comparatively rapid temperature decrease towards the center of the plate extends the speed slow down period, when $R_0 = 2.5$ to slightly past the center, and that it also has a depressing effect on u when $R = 0.75$. The higher temperature above then promotes an accelerating speed. In Fig. 4(b), we note that for the high starting speed ($R_0 = 2.5$) and comparatively rapid wall tem-

perature decrease there is developed a comparatively rapid boundary-layer thickening past the minimum temperature point. For the lower entry speed, ($R_0 = 0.75$), the boundary layer is generally thinner with the maximum thickness point closer to the center and there is the temporary slow speed thinning effect of the starting position.

The isotherms, Figs. 4(d) and (e), are wavy as one would expect and gradually lose this waviness as the outer layers are approached. The isotherm bands (region between isotherms) show a maximum thickness along a line running approximately from the minimum wall temperature point to a point somewhat below the maximum thickness position of the boundary layer. It is rather interesting and somewhat surprising that the isotherm spacing at the slower entry speed is somewhat closer, and thus indicates greater heat transfer.

Case V

Figure 5(a) shows a speed curve for the starting condition $R_0 = 0.75$ with an essentially relatively high uniform speed change until the upper wall region is reached. Figures 5(b) and (c) are the streamline for the R_0 values 2.5 and 0.75, respectively. The streamline waviness noticed in other higher speed starting cases is also present here. Both boundary layers show retarded

growth in a region below the peak wall temperature position.

Figures 5(d) and (e) show the isotherms for this case. The isotherm strips do not have the central thickening observed for the Case IV. Here also the isotherms indicate a somewhat increased heat transfer for the smaller starting speed ($R_0 = 0.75$).

DIRECT COMPARISONS OF CASES IV AND V

Figure 6(a) shows a comparison in thickness for Cases IV and V at R_0 values of 2.5 and 0.75. It is interesting that they tend to a common

value toward the top of the plate. Figure 6(b) shows the comparison in R . For Case V, the curves for the starting R_0 's 2.5 and 0.75 approach early essential coincidence and show values near the standard $R = 1$ in the middle section of the plate. For Case IV, the R values differ markedly until the upper quarter of the plate is reached. There is no extended range of R values near 1.

Comparison of the heat-transfer coefficients are made in Fig. 6(c). One notes again that the flows with lower starting speeds have the higher heat transfer and as one would expect a higher

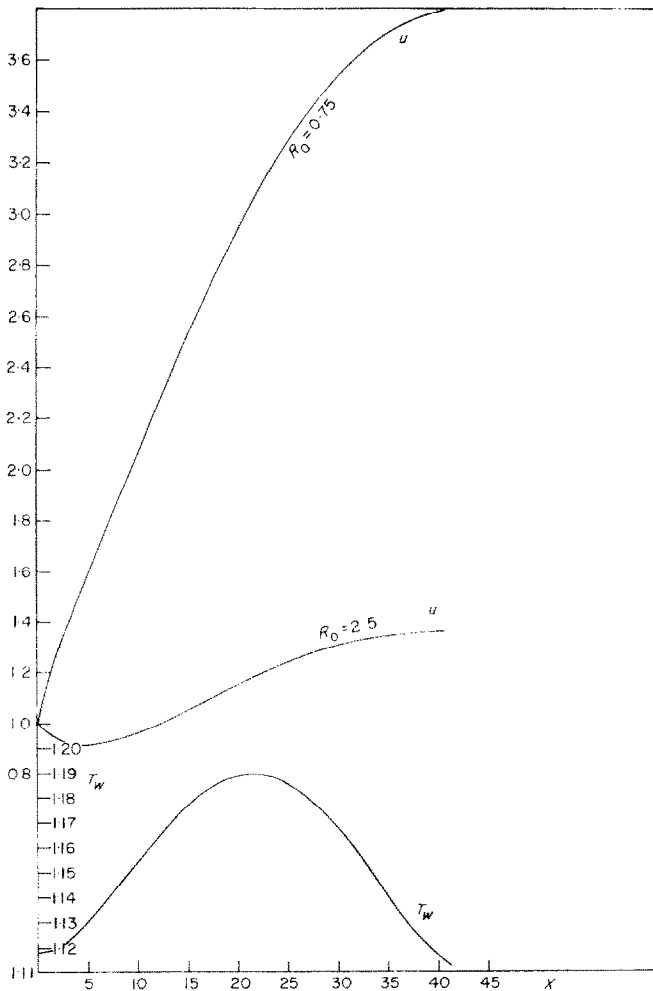


FIG. 5(a). Case V. Temperature and speed functions.

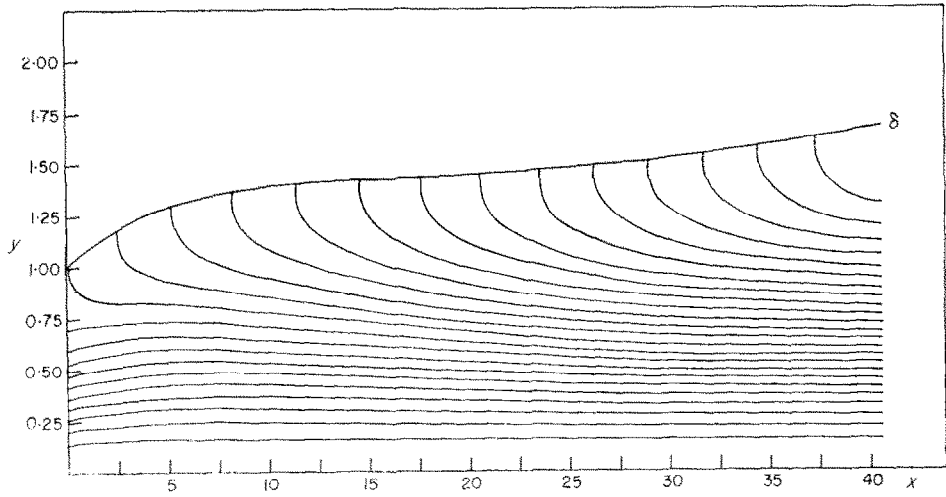


FIG. 5(b). Case V. Streamlines ($R_0 = 2.5$).

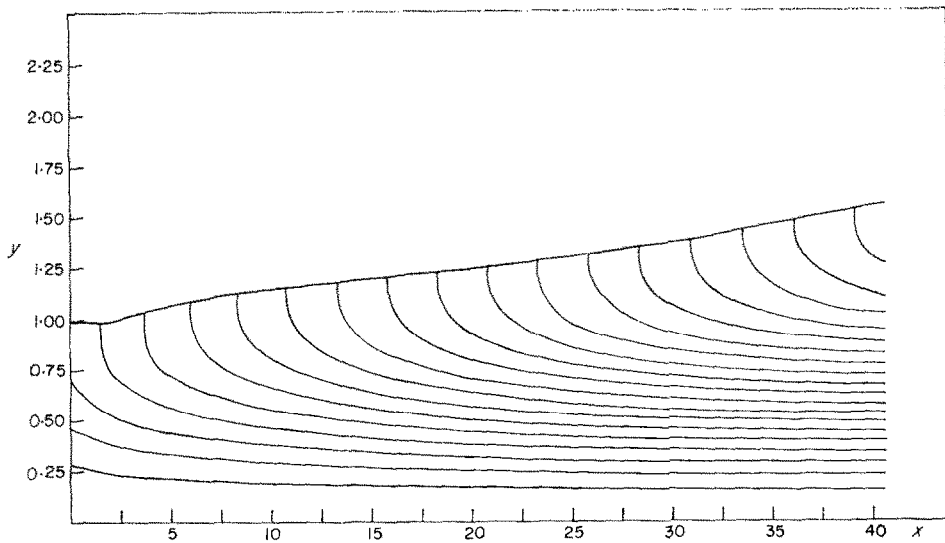


FIG. 5(c). Case V. Streamlines ($R_0 = 0.75$).

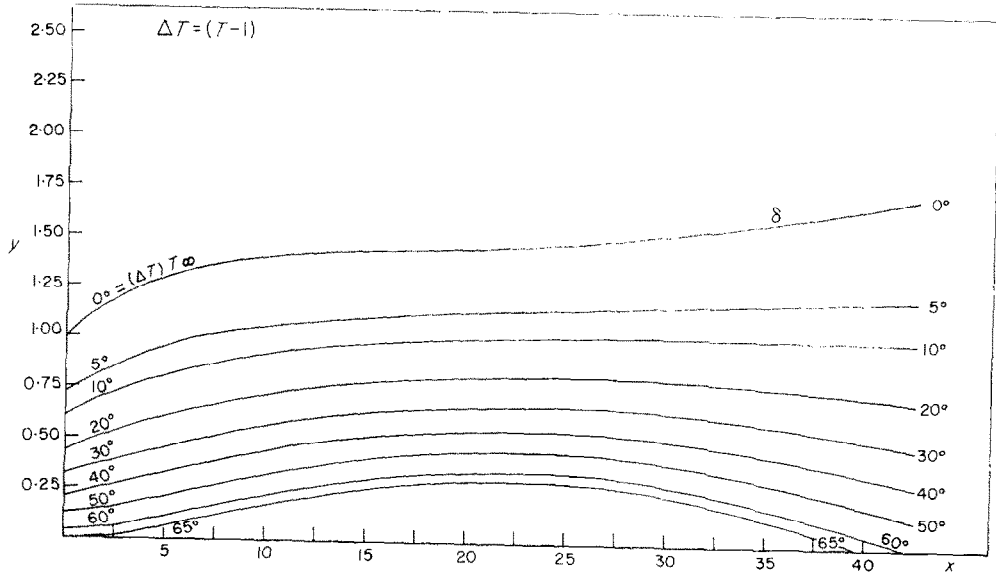


FIG. 5(d). Case V. Isotherms ($R_0 = 2.5$).

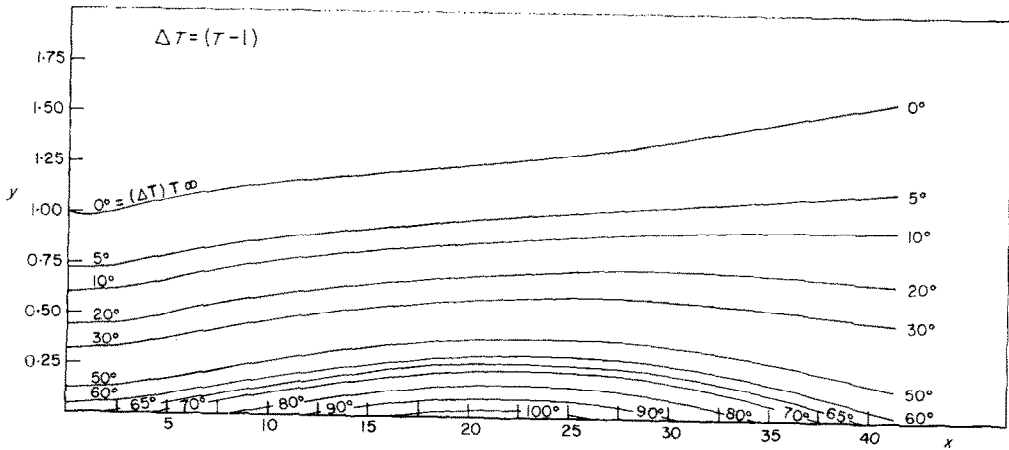


FIG. 5(e). Case V. Isotherms ($R_0 = 0.75$).

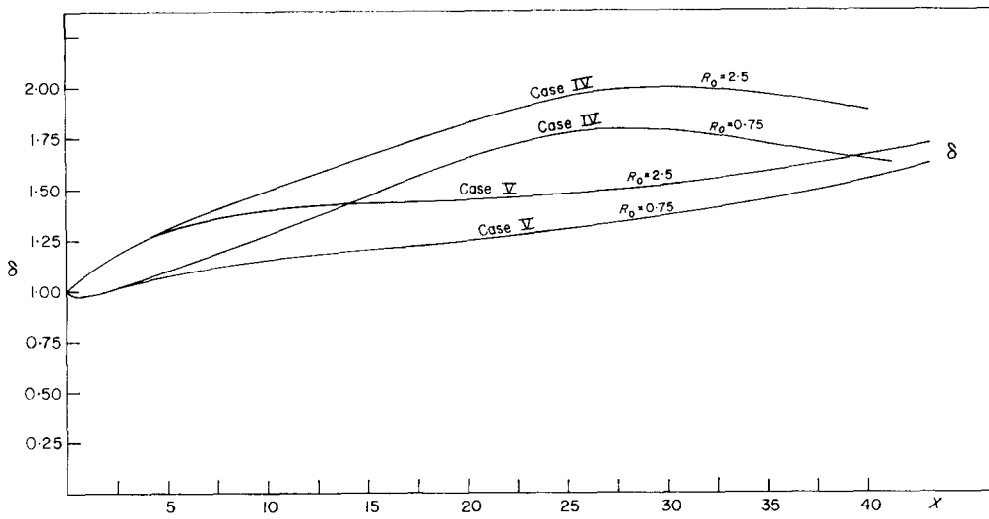


FIG. 6(a). Comparative thickness functions, cases IV and V.

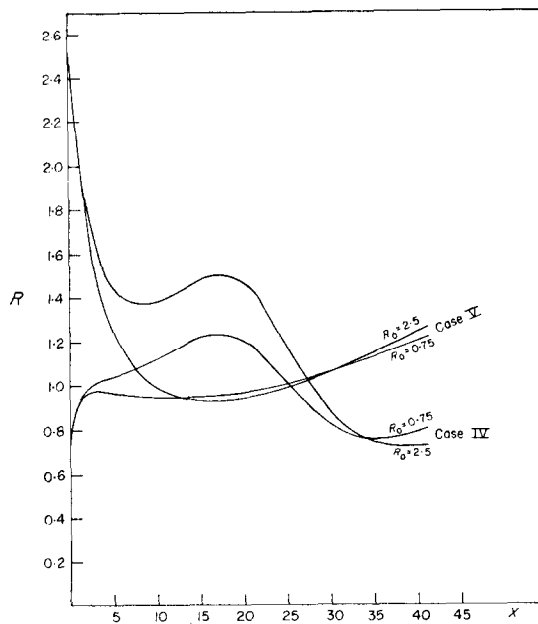


FIG. 6(b). Comparative R functions, cases IV and V.

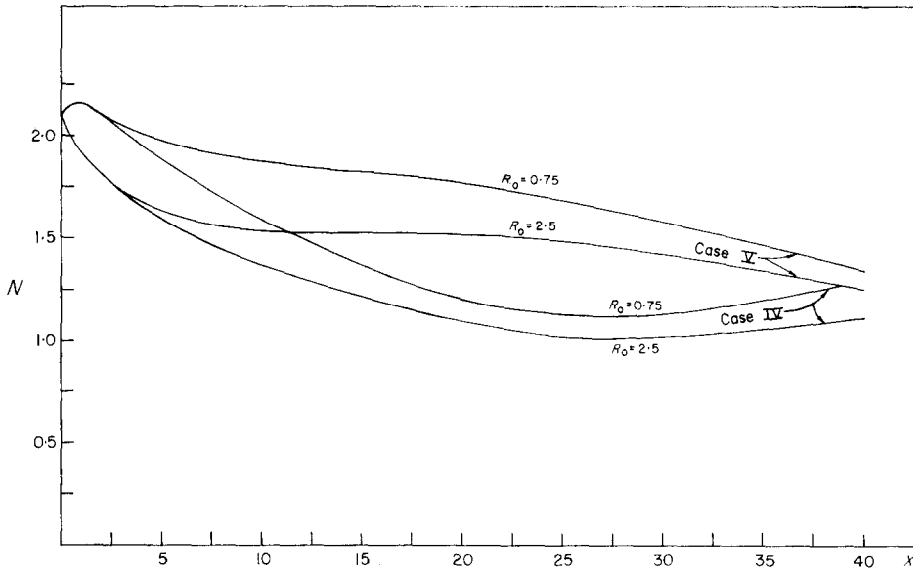


FIG. 6(c). Comparative heat-transfer coefficients, cases IV and V.

temperature wall condition generally also gives higher heat transfer.

Summary: The author has not succeeded in finding sufficient experimental results on which to check his theory. Generally, it may be said that the theoretical results indicate that for the variable wall temperature cases, the starting boundary conditions do affect the boundary-layer flow structure by more than just a displacement distance found for the constant temperature case.

ACKNOWLEDGEMENTS

The author wishes gratefully to acknowledge the very helpful check of the mathematical work and the use of the computing machines for the numerical results by Dr. Gertrude Blanch of our Applied Mathematics Research Laboratory.

REFERENCES

1. M. G. SCHERBERG, Natural convection near and above thermal leading edges on vertical walls, *Int. J. Heat Mass Transfer* **5**, 1001-1010 (1962).
2. S. GOLDSTEIN, *Modern Developments in Fluid Dynamics*, Vol. II, p. 641. Clarendon Press, Oxford (1938).
3. E. M. SPARROW and J. L. GREGG, Similar solutions for free convection from a nonisothermal vertical plate, *Trans. ASME*, **80**, 379 (1958).
4. R. C. HILL, An experimental investigation of free convection heat transfer from a nonisothermal vertical flat plate. University of California, Masters thesis (1961).
5. WERNER KRAUS, *Messung des Temperatur- und Geschwindigkeitsfeldes bei Freier Konvektion*. Verlag G. Braun, Karlsruhe (1955).
6. S. L. BARTOLSKY, Free convection heat transfer on a vertical plate under conditions of nonuniform surface temperature, Institute of Technology, USAF, W-PAFB, Masters thesis (1958).

Аннотация—Получены выражения для конвективного потока от вертикальных пластин, температура стенок которых произвольно ограничена. При этом найдено, что профили температуры и скорости в потоке подобны аналогично полученным в случае постоянной температуры стенки. Детально исследовано несколько случаев, в том числе случаи возрастания-уменьшения температуры стенки и наоборот. В результате получены линии тока, изотермы и распределения скоростей. Исследованы перенос тепла и влияние изменяющихся начальных условий на стенках.